DOI: 10.1021/ic900919w

Inorganic Chemistry
Article

New Heterometallic Carboxylate Frameworks: Synthesis, Structure, Robustness, Flexibility, and Porosity

Jie-Peng Zhang,*,†,‡ Sujit K. Ghosh,‡ Jian-Bin Lin,† and Susumu Kitagawa*,‡

†*MOE Key Laboratory of Bioinorganic and Synthetic Chemistry, School of Chemistry and Chemical Engineering, Sun Yat-Sen University, Guangzhou 510275, China, and* ‡*Department of Synthetic Chemistry and Biological Chemistry, Graduate School of Engineering, Kyoto University, Katsura, Nishikyo-ku, Kyoto 615-8510, Japan*

Received May 11, 2009

Solvothermal reactions of cobalt acetate, alkali metal hydroxide, and isophthalic acid (H_2ipa) in H_2O/alcohol produce five new three-dimensional (3D) heterometallic carboxylate frameworks, namely, $[Na_2Co(ipa)_2(MeOH)_2]_n$ (**1**), $[Na_2Co(ipa)_2(EtOH)_2]_n$ (**2**), $[Na_2Co(ipa)_2(H_2O)(EtOH)]_n$ (**3**), $[Li_2Co(ipa)_2(EtOH)]_n$ (**4**), and $\{[Li_2Co(ipa)_2(H_2O)]\cdot H_2O\}_n$ (**5**). Compounds **1**−**5** are all based on anionic $[Co(ipa)_2]_n$ square grids, which are linked by alkali metal ions in various manners to generate closely related but quite different 3D architectures. In addition to the carboxylate oxygen donors of the anionic $[Co(ipa)_2]_n$ square grids, the alkali metal ions are also coordinated by the MeOH, EtOH, or H_2O ligands. The prototypical compound **1** shows interesting solid-state structural transformations and sorption properties. The coordinated MeOH molecules in **1** can be easily substituted by moist H_2O, accompanying a structural transformation from the chiral phase **1** to centrosymmetric phase **3**. Further, thermal liberation of all MeOH ligands causes significant structural change and gives rise to a non-porous framework $[CoNa_2(ipa)_2]_n$ (**1′**), which adsorbs MeOH, EtOH, and MeCN but not acetone based on the sizes of solvent molecules. Moreover, **1′** can also selectively absorb CO_2 over N_2, H_2, and C_2H_2, demonstrating the importance of oxophilic Na(I) ion in controlling the gate-opening behavior.

Introduction

Porous coordination polymers (PCPs) or metal organic frameworks (MOFs) are a fast growing research topic for academic and industrial appeals.[1−8] Considerable efforts have been devoted to developing new structures and exploring novel properties, as well as rationalizing structure−property relationships. On the basis of the combination of metal ions and organic ligands, coordination polymers can be categorized into many subsets, which are different not only their chemical composition but also their synthetic chemistry, supramolecular structure, and porous properties.[9−26] For example, transition metal polypyridine frameworks are usually cationic unless the anions are also coordinated to the metal ions. Although extra-framework counterions always reduce the available pore volumes and usually block the

*To whom correspondence should be addressed. E-mail: zhangjp7@mail.sysu.edu.cn (J.-P.Z.), kitagawa@sbchem.kyoto-u.ac.jp (S.K.).

(1) Yaghi, O. M.; O'Keeffe, M.; Ockwig, N. W.; Chae, H. K.; Eddaoudi, M.; Kim, J. *Nature* **2003**, *423*, 705.
(2) Kitagawa, S.; Kitaura, R.; Noro, S. I. *Angew. Chem., Int. Ed.* **2004**, *43*, 2334.
(3) Bradshaw, D.; Claridge, J. B.; Cussen, E. J.; Prior, T. J.; Rosseinsky, M. J. *Acc. Chem. Res.* **2005**, *38*, 273.
(4) Kepert, C. J. *Chem. Commun.* **2006**, 695.
(5) Ma, L.; Abney, C.; Lin, W. *Chem. Soc. Rev.* **2009**, *38*, 1248.
(6) Perry, J. J. IV; Perman, J. A.; Zaworotko, M. J. *Chem. Soc. Rev.* **2009**, *38*, 1400.
(7) Murray, L. J.; Dincă, M.; Long, J. R. *Chem. Soc. Rev.* **2009**, *38*, 1294.
(8) Czaja, A. U.; Trukhan, N.; Müller, U. *Chem. Soc. Rev.* **2009**, *38*, 1284.
(9) Wang, M.-S.; Guo, G.-C.; Cai, L.-Z.; Chen, W.-T.; Liu, B.; iWu A.-Q.; Huang, J.-S. *Dalton Trans.* **2004**, 2230.
(10) Hu, S.; He, K.-H.; Zeng, M.-H.; Zou, H.-H.; Jiang, Y.-M. *Inorg. Chem.* **2008**, *47*, 5218.
(11) Li, G.; Zhu, C.-F.; Xi, X.-B.; Cui, Y. *Chem. Commun.* **2009**, 2118.
(12) Dong, Y.-B.; Zhang, Q.; Liu, L.-L.; Ma, J.-P.; Tang, B.; Huang, R.-Q. *J. Am. Chem. Soc.* **2007**, *129*, 1514.
(13) Zhang, X.-M.; Qing, Y.-L.; Wu, H.-S. *Inorg. Chem.* **2008**, *47*, 2255.
(14) Wang, Y.; Cheng, P.; Chen, J.; Liao, D.-Z.; Yan, S.-P. *Inorg. Chem.* **2007**, *46*, 4530.
(15) Du, M.; Jiang, X.-J.; Zhao, X.-J. *Inorg. Chem.* **2007**, *46*, 3984.
(16) Tang, E.; Dai, Y.-M.; Zhang, J.; Li, Z.-J.; Yao, Y.-G.; Zhang, J.; Huang, X.-D. *Inorg. Chem.* **2007**, *46*, 8490.
(17) Ouellette, W.; Yu, M. H.; O'Connor, C. J.; Hagrman, D.; Zubieta, J. *Angew. Chem., Int. Ed.* **2006**, *45*, 3497.
(18) Su, C.-Y.; Goforth, A. M.; Smith, M. D.; Pellechia, P. J.; zur Loye, H.-C. *J. Am. Chem. Soc.* **2004**, *126*, 3576.
(19) He, X.; Lu, C.-Z.; Yuan, D.-Q. *Inorg. Chem.* **2006**, *45*, 5760.
(20) He, J.; Zhang, J.-X.; Tsang, C.-K.; Xu, Z.-T.; Yin, Y.-G.; Li, D.; Ng, S.-W. *Inorg. Chem.* **2008**, *47*, 7948.
(21) Bai, Y.-L.; Tao, J.; Huang, R.-B.; Zheng, L.-S. *Angew. Chem., Int. Ed.* **2008**, *47*, 5344.
(22) Zhang, J.-P.; Chen, X.-M. *Chem. Commun.* **2006**, 1689.
(23) Wu, T.; Zhang, J.; Zhou, C.; Wang, L.; Bu, X.-H.; Feng, P.-Y. *J. Am. Chem. Soc.* **2009**, *131*, 6111.
(24) Wu, T.; Yi, B.-H.; Li, D. *Inorg. Chem.* **2005**, *44*, 1175.
(25) Shimizu, G. K. H.; Vaidhyanathan, R.; Taylor, J. M. *Chem. Soc. Rev.* **2009**, *38*, 1430.
(26) Férey, G. *Chem. Soc. Rev.* **2008**, *37*, 191.

Published on Web 07/15/2009

channel apertures, they may be utilized for ion exchange and increasing adsorption affinity.[27] Neutral transition metal carboxylate frameworks are the mainstream of PCPs for the rich availability of transition metal carboxylate clusters and polycarboxylate ligands. Carboxylates and pyridines can be also combined as mixed ligands to offer additional structural diversity.[28,29] Recently, metal azolate frameworks have received great attention because azolate ligands combine the predictable coordination behavior of pyridines and the negative charge of carboxylates.[22−24] The strong bonding between transition metal ions and azolate ligands also facilitate structure control and high framework stability.[22]

Besides pore size and shape, surface characteristic is an important feature in controlling porous functionalities. Introducing coordinatively unsaturated metal centers (UMCs) on the pore surface of PCPs has been emerging as one of the most promising strategies for enhancing adsorption affinity and catalytic ability.[30] As common divalent transition metal ions usually prefer the saturated, octahedral coordination geometry, it is generally hard to obtain a UMC. To rationally immobilize a UMC and fabricate novel functionalities, other metal ions such as lanthanides, coinage metal ions, and alkali metal ions have been studied since they offer very flexible coordination geometries and different chemical properties as compared to the divalent transition metal ions.[31−41] Compared to lanthanides and coinage metal ions, alkali metal ions are not common building blocks in coordination chemistry, and usually cannot be used alone to construct homometallic open frameworks with sufficient stability. To solve this problem, transition metal ions could be incorporated to build a heterometallic framework.[35−41] Nevertheless, such kinds of heterometallic coordination polymers have been rarely studied as porous materials, albeit alkali metal ions may have advantages in providing special host−guest interaction, high framework flexibility, and low framework density.

Combining Na(I) or Li(I) with Co(II) and isophthalate (ipa^{2-}), we have successfully constructed a new series heterometallic carboxylate frameworks under solvothermal conditions. The structures of these new compounds are highly correlated, showing robustness and flexibility of the coordination frameworks. Moreover, framework robustness and flexibility have been demonstrated by the prototypical architecture, in which the coordinated solvent molecules can be substituted and/or removed to produce significant structural transformations and interesting porous properties.

Experimental Section

Materials and Physical Measurements. Commercially available reagents (AR) are used as received without further purification. Thermogravimetric analysis is carried out with Rigaku TG8120 in nitrogen atmosphere. X-ray powder diffraction data are collected on a Rigaku RINT-2200HF (Ultima) or a D/M-2200T automated diffractometer with Cu Kα radiation. Gas sorption isotherms are measured by an Autosorb-1-C or a Belsorp MAX volumetric adsorption equipment. Solvent vapor sorption isotherms are measured by a Belsorp 18 volumetric adsorption equipment.

Synthesis of $[Na_2Co(ipa)_2(MeOH)_2]_n$ (1). A mixture of $Co(OAc)_2\cdot 4H_2O$ (0.125 g, 0.5 mmol), H_2ipa (0.166 g, 1.0 mmol), NaOH (0.050 g, 1.2 mmol), MeOH (6.0 mL), and H_2O (0.5 mL) was sealed in a Teflon-lined autoclave and heated at 120 °C for 3 days to give violet crystals **1** (yield ca. 60%).

$[Na_2Co(ipa)_2(EtOH)_2]_n$ (2) and $[Na_2Co(ipa)_2(H_2O)(EtOH)]_n$ (3). The reaction is carried out with the same method as for **1**, but MeOH is replaced by EtOH (6.0 mL). Violet crystals of **3** are obtained in about 50% yield, but usually contain small amounts of **2**.

$[Li_2Co(ipa)_2(EtOH)]_n$ (4). The reaction is carried out in the same method as for **1**, but NaOH is replaced by LiOH (0.024 g, 1.0 mmol), and MeOH is replaced by EtOH (6.0 mL). Violet crystals of **4** are obtained in about 50% yield with small amounts of intractable impurities.

$\{[Li_2Co(ipa)_2(H_2O)]\cdot H_2O\}_n$ (5). The reaction is carried out in the same method as for **1**, but NaOH is replaced by LiOH (0.024 g, 1.0 mmol), and MeOH is replaced by iPrOH (6.0 mL). Violet crystals **5** are obtained in about 40% yield with small amounts of intractable impurities.

X-ray Crystallography. Data collections are performed with Mo Kα radiation on a Rigaku mercury (**1**−**4**) or a Bruker Apex (**5**) CCD diffractometer. The structures are solved by direct methods and all non-hydrogen atoms are refined anisotropically by least-squares on F^2 using the SHELXTL program.[42] Hydrogen atoms on organic ligands are generated by the riding mode.

Results and Discussion

Synthesis. Five new coordination polymers, that is, $[Na_2Co(ipa)_2(MeOH)_2]_n$ (**1**), $[Na_2Co(ipa)_2(EtOH)_2]_n$ (**2**), $[Na_2Co(ipa)_2(H_2O)(EtOH)]_n$ (**3**), $[Li_2Co(ipa)_2(EtOH)]_n$ (**4**), and $\{[Li_2Co(ipa)_2(H_2O)]\cdot H_2O\}_n$ (**5**) have been successfully synthesized by solvothermal reactions of $Co(OAc)_2$, H_2ipa, and NaOH or LiOH in mixed H_2O/alcohol solvents. Solvothermal reactions of transition metal salt, carboxylic acid, and alkali hydroxide in mixed H_2O/alcohol have been proven to be an effective synthetic strategy for preparation of heterometallic PCPs containing both alkali and transition metal ions. Two related PCPs with similar alkali-cobalt-isophthalate compositions have been reported previously. Livage et al. showed that solvothermal reaction of $CoSO_4$, H_2ipa, and NaOH in H_2O/EtOH at 180 °C yield $[Na_3Co_6O(OH)(ipa)_6]\cdot H_2O$ (MIL-104) without an active metal center.[37] Chen et al. used the solvothermal reaction of $Co(OAc)_2$, H_2ipa, and

(27) Liu, Y.; Eubank, J. F.; Cairns, A. J.; Eckert, J.; Kravtsov, V. C.; Luebke, R.; Eddaoudi, M. *Angew. Chem., Int. Ed.* **2007**, *46*, 3278.
(28) Dybtsev, D. N.; Chun, H.; Kim, K. *Angew. Chem., Int. Ed.* **2004**, *43*, 5033.
(29) Lan, A.; Li, K.; Wu, H.; Olson, D. H.; Emge, T. J.; Ki, W.; Hong, M.-C.; Li, J. *Angew. Chem., Int. Ed.* **2009**, *48*, 2334.
(30) Dincă, M.; Long, J. R. *Angew. Chem., Int. Ed.* **2008**, *47*, 6766.
(31) Guo, X.-D.; Zhu, G.-S.; Li, Z.-Y.; Sun, F.-X.; Yang, Z.-H.; Qiu S.-L. *Chem. Commun.* **2006**, 3172.
(32) Chen, B.; Yang, Y.; Zapata, F.; Lin, G.; Qian, G.; Lobkovsky, E. B. *Adv. Mater.* **2007**, *19*, 1693.
(33) Zhao, J.; Long, L.-S.; Huang, R.-B.; Zheng, L.-S. *Dalton Trans.* **2008**, 4717.
(34) Zhang, J.-P.; Kitagawa, S. *J. Am. Chem. Soc.* **2008**, *130*, 907.
(35) Xiang, S.-C.; Wu, X.-T.; Zhang, J.-J.; Fu, R.-B.; Hu, S.-M.; Zhang, X.-D. *J. Am. Chem. Soc.* **2005**, *127*, 16352.
(36) Horike, S.; Matsuda, R.; Tanaka, D.; Mizuno, M.; Endo, K.; Kitagawa, S. *J. Am. Chem. Soc.* **2006**, *128*, 4222.
(37) Livage, C.; Guillou, N.; Chaigneau, J.; Rabu, P.; Drillon, M.; Férey, G. *Angew. Chem., Int. Ed.* **2005**, *44*, 6488.
(38) Cheng, X.-N.; Zhang, W.-X.; Lin, Y.-Y.; Zheng, Y.-Z.; Chen, X.-M. *Adv. Mater.* **2007**, *19*, 1494.
(39) Yang, S.; Lin, X.; Blake, A. J.; Thomas, K. M.; Hubberstey, P.; Champness, N. R.; Schröder, M. *Chem. Commun.* **2008**, 6108.
(40) Mulfort, K. L.; Farha, O. K.; Stern, C. L.; Sarjeant, A. A.; Hupp J. T. *J. Am. Chem. Soc.* **2009**, *131*, 3866.
(41) Wu, J.-Y.; Ding, M.-T.; Wen, Y.-S.; Liu, Y.-H.; Lu, K.-L. *Chem.—Eur. J.* **2009**, *15*, 3604.
(42) *SHELXTL 6.10*; Bruker Analytical Instrumentation: Madison, WI, 2000.

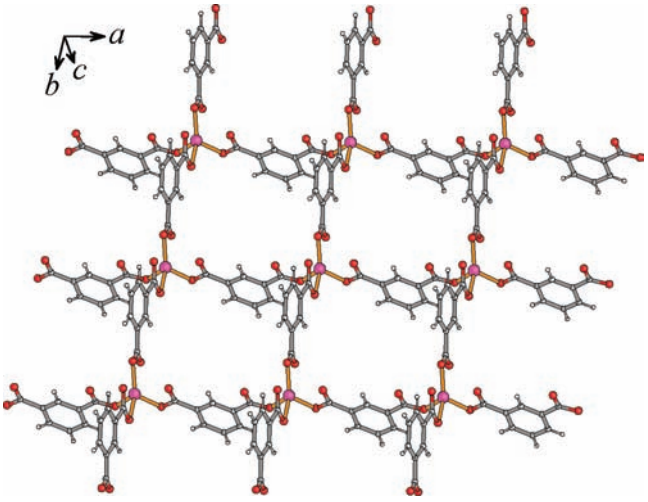

Figure 1. Perspective view of the anionic $[Co(ipa)_2]_n$ square-grid of **1**.

KOH in H_2O/MeOH at 160 °C to get $[KCo_7(OH)_3(ipa)_6(H_2O)_3]\cdot 12H_2O$ (MCF-17), in which both the K(I) and Co(II) ions can be activated by thermal liberation of the coordinated solvent molecules.[38] The main differences of the synthetic conditions among MIL-104, MCF-17, and **1**−**5** are the reactant stoichiometry and reaction temperature. The reaction outcome is also sensitive to the composition of the mixed H_2O/alcohol solvents. Probably because of the high coordination affinity between alkali metal ions and H_2O, alkali metal ions cannot be incorporated into the coordination polymers when H_2O concentrations are high, while low H_2O concentrations lead to a large quantity of insoluble impurities mainly composed of alkali metal salts. Furthermore, the resulted solids usually contain several crystalline products and/or impurities. These results exemplify the rich chemical composition and structures of this heterometallic carboxylate system. Nevertheless, we have optimized the reaction condition to obtain the phase-pure **1**.

Structure. The coordination polymer **1** crystallizes in the chiral space group $P4_1$, containing one Co(II), two Na(I), two ipa^{2-}, and two MeOH in the asymmetric unit (Supporting Information, Figure S1). The Co(II) center is coordinated by four carboxylate groups from four different ipa^{2-} ligands, which behave in typical monodentate or quasi-bidentate chelating modes (short Co−O 1.994−2.094 Å, long Co−O 2.312−3.059 Å). The four strong Co−O bonds define a tetrahedral coordination geometry. As each ipa ligand coordinates to two Co(II) along the *a*- or *b*-axis, the interconnection produce an anionic, regular, square-grid $[Co(ipa)_2]_n$ network (Co···Co 9.966 Å, Co···Co···Co 90°) extended through the *ab*-plane (Figure 1). The aromatic planes of ipa^{2-} are perpendicular to the grid (parallel to the *c*-axis), giving a thick (11.6 Å, van der Waals radii of corresponding atoms have been considered) bilayer structure with large unoccupied spaces, in which two perpendicular sets of slits (6.8×4.0 Å^2) running along the *a*- or *b*-axis are joined by square windows in the *c*-axis (6.8×6.8 Å^2). Obviously, the $Co(O_2CR)_4$ coordination geometry in **1** is not energetically favored, which is stabilized by further coordination with Na(I) ions. Two adjacent $Co(O_2CR)_4$ moieties from two adjacent bilayers are connected by two kinds of octahedrally coordinated

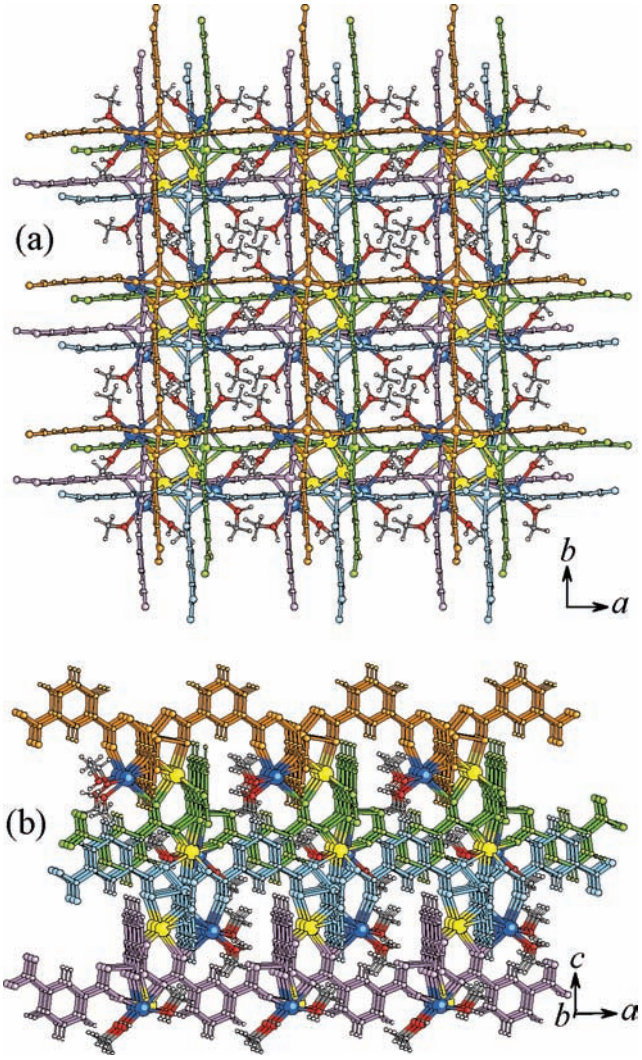

Figure 2. Top (a) and side (b) views of the 3D structure of **1** showing the packing fashion of adjacent $[Co(ipa)_2]_n$ bilayers (four bilayers are highlighted by different colors) and connection with Na(I) ions (inner: yellow, outer: blue).

Na(I) ions (Supporting Information, Figure S1), in which the inner one (Na1) is completely surrounded by six carboxylate oxygen atoms, while the outer one (Na2) is coordinated by four carboxylate oxygen atoms and two hydroxyl oxygen atoms from MeOH (in a *cis*-configuration). Consequently, adjacent $[Co(ipa)_2]_n$ bilayers are glued by Na(I) ions along the *c*-axis into a neutral three-dimensional (3D) framework. Besides the coordination with Na(I) ions, adjacent $[Co(ipa)_2]_n$ bilayers also interdigitate with close face-to-face $\pi-\pi$ interactions (3.4 Å). The degree of interdigitation can be estimated by comparing the bilayer thickness (11.6 Å) and the interlayer separations (5.1 Å). According to the unique shape of bilayer structure, each bilayer undergoes 90° rotation and a certain offset from its neighbor to accomplish efficient packing. Since the grid size is larger than twice the thickness of a benzene ring, 3D intersecting, narrow channels (*d* 3.2 Å) are retained after interdigitation (Figure 2). Nevertheless, these channels (void 25.9%) are occupied by the coordinated MeOH molecules, and no solvent accessible volume can be found in the crystal structure of **1**. Similar structures have been observed in the isostructural

Table 1. Crystallographic Data and Refinement Parameters

	1	2	3	4	5
formula	$C_{18}H_{16}CoNa_2O_{10}$	$C_{20}H_{20}CoNa_2O_{10}$	$C_{18}H_{16}CoNa_2O_{10}$	$C_{18}H_{14}CoLi_2O_9$	$C_{16}H_{12}CoLi_2O_{10}$
FW	497.22	525.27	497.22	447.10	437.07
T/K	113(2)	113(2)	113(2)	113(2)	293(2)
space group	$P4_1$	$P4_1$	$P2_1/n$	$P2_1/n$	$C222_1$
a/Å	9.9660(9)	10.0292(8)	10.896(2)	10.662(2)	12.024(3)
b/Å	9.9660(9)	10.0292(8)	14.256(2)	12.215(2	15.032(4)
c/Å	20.472(2)	20.808(2)	13.901(3)	14.466(3)	12.948(3)
β/deg	90	90	109.49(3)	108.73(3)	90
V/Å^3	2033.3(3)	2093.0(3)	2035.6(7)	1784.3(6)	2340.5(9)
Z	4	4	4	4	4
D_c/g cm^{-3}	1.624	1.667	1.622	1.664	1.240
μ/mm^{-1}	0.941	0.919	0.940	1.014	0.774
R_1 ($I > 2\sigma$)	0.0506	0.0434	0.0572	0.0420	0.0455
wR_2 (all data)	0.1142	0.0969	0.1213	0.0967	0.1165
GOF	1.045	1.048	1.032	1.047	1.067
Flack parameter	0.00(2)	0.00(2)			0.10(3)

$NH_2(CH_3)_2[NaM(ipa)_2]$ (M = Cd or Co),[43] which also contain similar anionic $[M(ipa)_2]_n$ square grids linked by Na(I) ions. However, their final 3D frameworks are anionic because each pair of $M(O_2CR)_4$ moieties are linked by only one Na(I) ion, which is completely coordinated by carboxylates, excluding any coordinated solvent molecules.

Replacing the MeOH molecules in **1** with EtOH produces an isostructural compound **2** (Supporting Information, Figure S2). To accommodate the larger EtOH molecules, the crystal lattice is slightly expanded (Table 1), which can be ascribed to the distortions of coordination geometries (M−O distance variations 0.1−0.2 Å). The coordinated EtOH molecules occupy about 29.2% of the crystal volume.

The coordinated solvent molecules in **1**/**2** can be also replaced by mixed H_2O/EtOH to give a centrosymmetric ($P2_1/n$) analogue **3**, which possesses a slightly distorted square-grid $[Co(ipa)_2]_n$ bilayer structure. However, the local coordination environments of **3** (Supporting Information, Figure S3) are obviously different from those of **1**/**2**. Some of the carboxylate groups change the coordination modes from monodentate to quasi-bidentate or conversely to coordinate with Co(II). Although the Na(I) ions possess similar octahedral coordination environments, they are located in very different positions. For example, each interlayer connection between two $Co(O_2CR)_4$ moieties in **1**/**2** is uniformly provided by an inner and an outer Na(I) ions (Figure 2), and each kind of Na(I) ion form a 4_1 helix along the bilayer packing direction (*c*-axis) with equal interatomic separations (inner 5.58 Å, outer 7.02 Å). However, half interlayer $Co(O_2CR)_4$ moieties in **3** are only joined by an inner Na(I) ion (Na3), while another half are joined by an inner (Na1) and two outer Na(I) ions (Na2) (Figure 3 and Supporting Information, Figure S3). Consequently, the outer Na(I) ions in **3** exhibit as isolated dimers (intradimer Na···Na 6.63 Å, interdimer Na···Na 10.90 Å), but the inner Na(I) ions of **3** are arranged in a straight fashion (Na···Na 5.45 Å). Moreover, the interlayer offset directions in **1**/**2** and **3** follow a 4_1 helical and a zigzag fashion, respectively, while common observed ones for two-dimensional (2D) coordination polymers are unidirectional. Nevertheless, the $[Na_2Co(ipa)_2]_n$ framework of **3** also contains 3D intersecting narrow channels

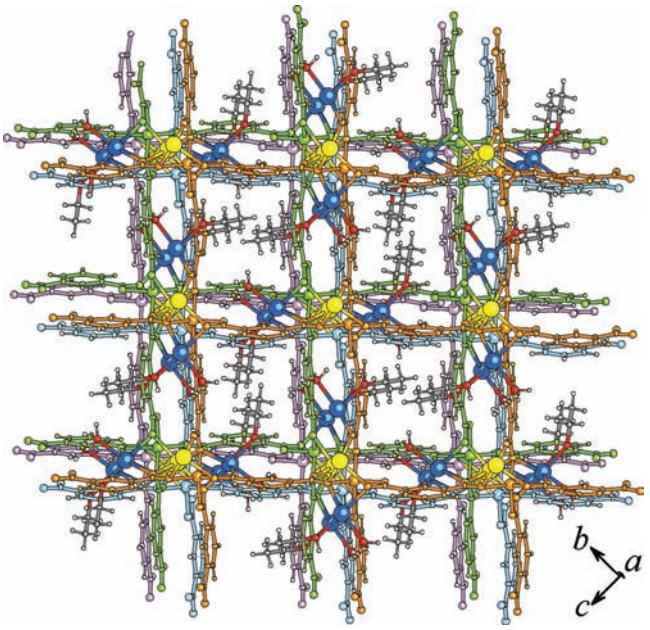

Figure 3. Perspective view of the 3D structure of **3** (color codes follow Figure 2).

(*d* 2.9 Å, void 24.6%), which are occupied by the coordinated H_2O and EtOH molecules.

The Li(I)−Co(II) heterometallic caboxylate **4** and **5** are also composed of alkali metal ion connected $[Co(ipa)_2]_n$ bilayers. Because of the small radius and low coordination number of Li(I), the local coordination environments in **4**/**5** are significantly different from those in **1**−**3**, which can be judged by the coordination geometries of the $Co(O_2CR)_4$ moieties (Supporting Information, Figure S4 and S5), the shape of the $[Co(ipa)_2]_n$ bilayers, and the connection modes of the bilayers. Compared to the regular square grids in **1**−**3**, the $[Co(ipa)_2]_n$ bilayers in **4** and **5** are distorted as rhombic grids (Figure 4 and 5).

In compound **4**, the aromatic rings are not perpendicular to the bilayer plane, reducing the thickness of the bilayer. While the bilayer packing manner is similar to that in **3**, half interlayer connection between $Co(O_2CR)_4$ moieties in **4** are provided by a pair of inner Li(I) ions, and another half are provided by a pair of outer ones, which is different from those of **1**−**3**. After connecting the bilayers

(43) Che, G.-B.; Liu, C.-B.; Wang, L.; Cui, Y.-C. *J. Coord. Chem.* **2007**, *60*, 1997.

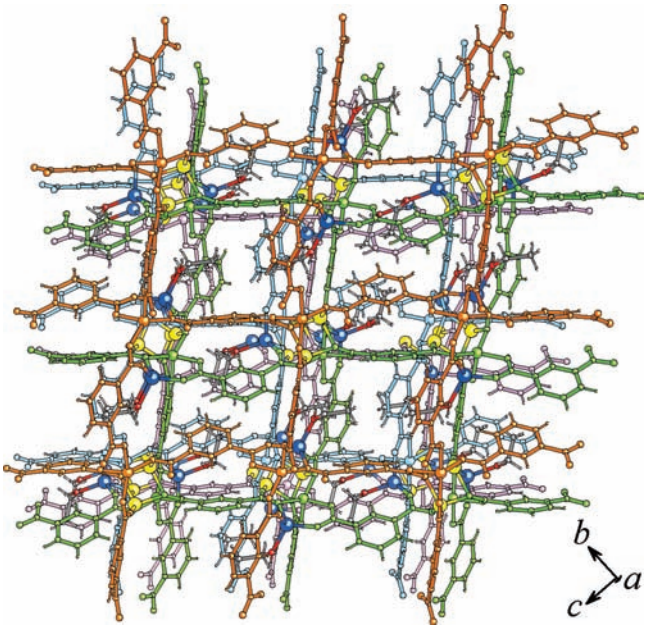

Figure 4. Perspective view of the 3D structure of **4** (color codes follow Figure 2).

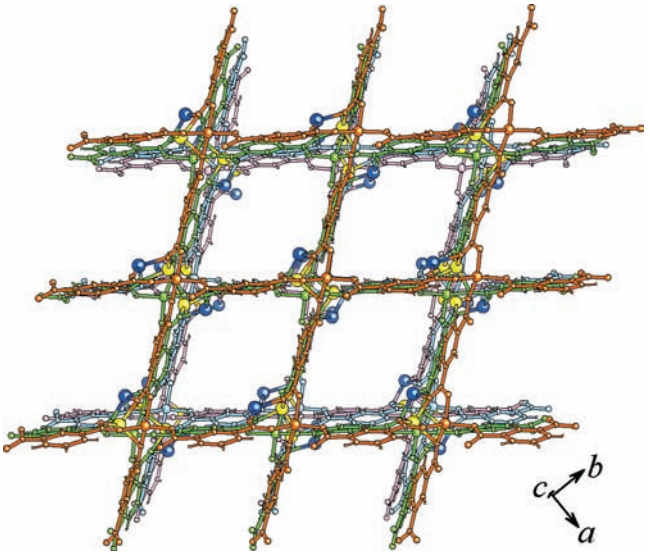

Figure 5. Perspective view of the 3D $[Li_2Co(ipa)_2]$ framework of **5** (color codes follow Figure 2).

by Li(I) ions, the $[Li_2Co(ipa)_2]_n$ framework of **4** only contains small and isolated cavities (16.7%), which are occupied by the coordinated EtOH molecules (Figure 4).

The aromatic rings in **5** are almost perpendicular to the bilayer plane. The bilayers in **5** adopt a basically eclipsed fashion, which is different from the complicated ones in **1**−**4**. Consequently, the $[Li_2Co(ipa)_2]_n$ framework exhibits large 1D channels (Figure 5), which are occupied by not only the coordinated but also the guest H_2O molecules.

Solid-State Transformation. Apparently, pure **1** can be synthesized in high yield. However, a satisfactory XRPD pattern for **1** can be only obtained by protecting the as-synthesized sample in its mother liquor or saturated MeOH vapor. Once the as-synthesized sample is exposed in air, additional XRPD peaks are evident. After

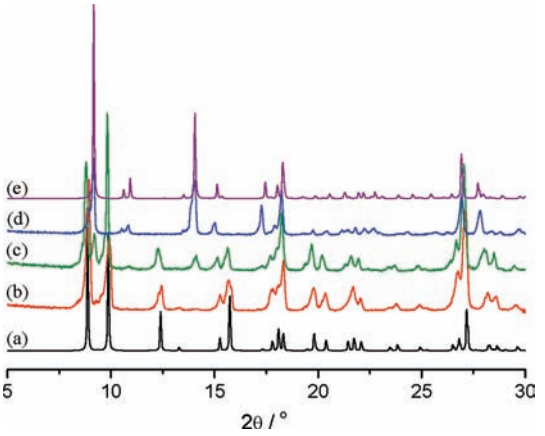

Figure 6. XRPD patterns of simulated **1** (a), as-synthesized **1** (b), **1** exposed in air for 10 min (c), **1** exposed in air for 1 day (d), and simulated **3** (e).

prolonged exposure in air, **1** completely transforms to another new crystalline phase. Although a single crystal is not available,[44] the new phase displays a very similar XRPD pattern as for **3** (Figure 6), indicating a structural transformation from the chiral tetragonal phase to the centrosymmetric monoclinic one. Obviously, compound **1** cannot transform to compound **3** in air because the latter contains coordinated EtOH molecules. Actually, the change in XRPD patterns should be only understood as a transition to phase **3**, whose structure is highly related to the known compound **3**. This phase transition is probably caused by either removal of the coordinated MeOH molecules or substitution of the MeOH by atmospheric H_2O molecules, which should induce a framework contraction as observed in the structures of **1**−**3**. Comparing the crystal structures of **1** and **3** shows that the phase transition involves multiple, drastic structural transformations. The distortion of the anionic $[Co(ipa)_2]_n$ bilayers can be generated by changing the Co−O distances without significant coordination bond reconstruction. However, adjacent $[Co(ipa)_2]_n$ bilayers must shift their relative positions to alter the 4_1 helical interlayer offset fashion to the zigzag one. More remarkably, the Na(I) ions, at least the outer ones, must undergo bond breakages and reformations to accomplish their redistributions (Figure 7). While the inner Na(I) ions are completely coordinated by six carboxylate oxgens in an inert environment, the outer ones are coordinated by four carboxylate oxgens and two solvent oxygens as active centers. Removing the solvent molecules from the coordination sphere should give rise an unstable metal center, which can be compensated by further structural transformation to a more stable configuration.

Thermogravimetric analysis for **1** shows obvious weight loss at relatively low temperatures, but complete removal of the MeOH molecules occurs at about 130 °C (Supporting Information, Figure S6). Therefore, partial removal or substitution of the MeOH ligands should be also considered. To verify which mechanism is responsible for the structural transformation, we further examined the framework stability or transition by temperature-dependent XRPD, which revealed three main

(44) Vittal, J. J. *Coord. Chem. Rev.* **2007**, *251*, 1781.

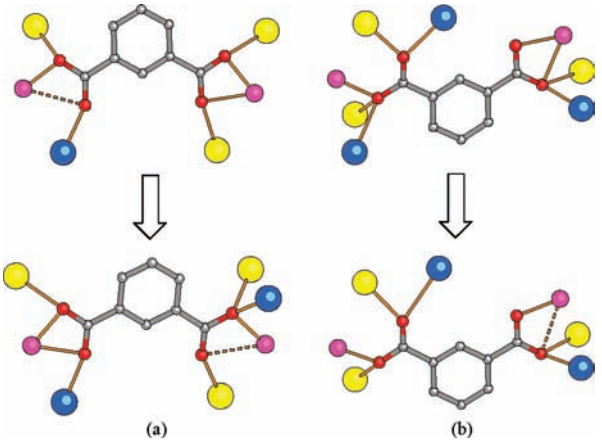

Figure 7. Changing of Coordination modes of the two crystallographically independent ipa^{2-} ligands (a and b) from **1** to **3** (pink, cobalt; yellow, inner sodium; blue, outer sodium).

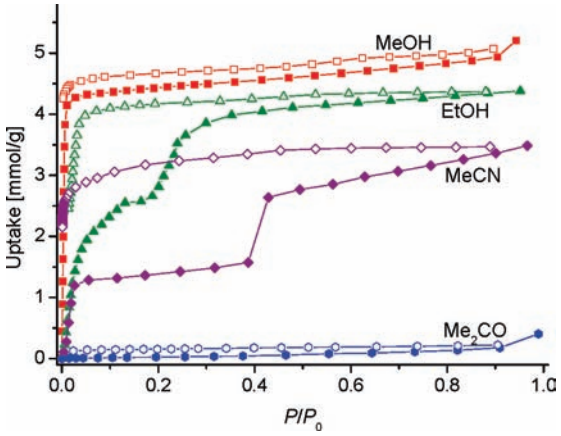

Figure 8. Adsorption (solid) and desorption (open) isotherms of MeOH, EtOH, MeCN, and acetone for **1′** at 298 K (P_0 is the saturation vapor pressure).

temperature-dependent phases. The "stable" phase **3** can be only retained up to 50 °C, while the second and third phases appear at 70 and 130 °C, respectively (Supporting Information, Figure S7). By keeping the sample in nitrogen, the high-temperature phase can be retained at room temperature. Phase **3** can be only recovered by subsequent exposure of the high temperature phase in air, indicating that moisture H_2O is necessary for phase **3**. These observations demonstrate that the two transitions originate from partial and complete removal of the coordinated ligands, respectively. In other words, the phase transitions observed in temperature-dependent XRPD are guest-induced rather than temperature induced. Therefore, the phase transition from **1** to **3** should be caused by the substitution of MeOH by atmospheric H_2O, since guest free $[Na_2Co(ipa)_2]_n$ (**1′**) is not stable in moist air. Although the exact amount of H_2O needed for the transition can be hardly measured, we did observe that the transition is accelerated as relative humidity increases. Additionally, it is reasonable to assume that **1′** is close packed, although its structure, that is, the high temperature phase, has not been solved. Nevertheless, because of the coordination flexibility of the metal ions and carboxylate ligands, the $[Na_2Co(ipa)_2]_n$ framework displays very interesting, multiple structural transformations triggered by ligand exchange and removal.[45−47]

Sorption Properties. Although **1′** should have smaller channel size and pore volume than for **1** (*d* 3.2 Å, void 25.9%) and **3** (*d* 2.9 Å, void 24.6%), guest sorption property is still possible considering the structural flexibility of the $[Na_2Co(ipa)_2]_n$ framework. To study the potential porosity of **1′**, sorption isotherms have been measured for solvent vapors including MeOH, EtOH, MeCN, and acetone, and gases including N_2, H_2, CO_2, and C_2H_2.

As shown in Figure 8, **1′** can adsorb large amounts of MeOH and EtOH, which are consistent with the formulas of **1** and **2** predicted by crystal structures. XRPD measurements also confirmed the recovery of **1** and **2** after adsorption of MeOH and EtOH, respectively. More information can be evaluated from the sorption isotherms. The MeOH adsorption isotherm shows a steep increase at the very low relative P/P_0 region, and saturation is almost achieved at $P/P_0 = 0.01$, indicating extremely strong host−guest interactions, which is ascribed to the fact that MeOH behaves as a coordinated ligand. There is essentially no desorption of MeOH at $P/P_0 > 0.003$, confirming that the phase transition from **1** to **3** is not because of the removal of MeOH. Although multiple phase transitions from **1′** to **1** are expected during the adsorption of MeOH, no obvious step can be identified from the adsorption isotherm, which may be ascribed to the extremely low gating pressure induced by the strong adsorption. In contrast, the EtOH isotherm is less steep and displays an obvious step near the uptake of 1 EtOH molecule per formula unit. According to the stoichiometry, the plateau may be assigned to the less opening phase **3**. However, the phase transitions from **1′** to **3**, both for MeOH and EtOH, might occur at the initial stages of adsorption.

While readsorption of the original solvent vapors is quite normal as expected,[45−47] **1′** can adsorb other "*foreign*" guests. At $P/P_0 < 0.025$, the MeCN isotherm almost traces that for EtOH, after that it reaches a plateau near the uptake of 0.5 MeCN per formula unit. The MeCN uptake remains almost unchanged until $P/P_0 = 0.38$, at which the uptake suddenly increases to 1.0 MeCN per formula unit, and further increases to 1.5 MeCN per formula unit gradually. The half integral uptake ratios indicate that the MeCN, whose affinity to Na(I) is weaker than for H_2O, MeOH, or EtOH, also forms coordination bonds with the host, but its binding behavior (e.g., strength and periodicity) should be different from the oxygen containing molecules. Both EtOH and MeCN desorption isotherms demonstrate that the last coordinated solvent molecule coordinated to the $[Na_2Co(ipa)_2]_n$ framework can be hardly removed at room temperature. Although acetone has a larger affinity to Na(I) than for MeCN, it is completely excluded by **1′** because of the larger molecular size.

The gas sorption isotherms of **1′** were depicted in Figure 9. N_2 and H_2 adsorption measurements at 77 K

(45) Ghosh, S. K.; Zhang, J.-P.; Kitagawa, S. *Angew. Chem., Int. Ed.* **2007**, *46*, 7965.
(46) Ghosh, S. K.; Bureekaew, S.; Kitagawa, S. *Angew. Chem., Int. Ed.* **2008**, *47*, 3403.
(47) Ghosh, S. K.; Kaneko, W.; Kiriya, D.; Ohba, M.; Kitagawa, S. *Angew. Chem., Int. Ed.* **2008**, *47*, 8843.

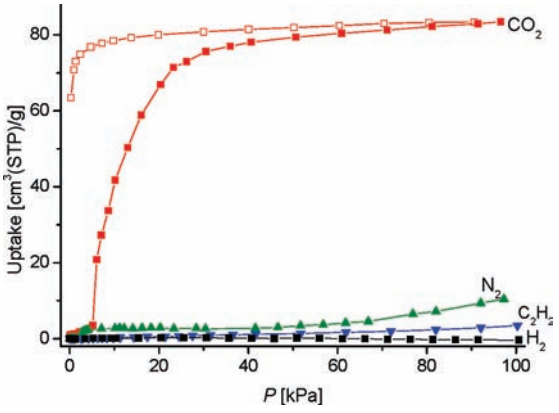

Figure 9. Sorption isotherms of N_2, H_2, CO_2, and C_2H_2 for **1′**.

reveal non-porous structure as expected from the structural analyses. However, **1′** shows a rather interesting CO_2 sorption isotherm at 195 K. The CO_2 uptake is negligible below 5 kPa, after which it suddenly increases and almost reaches the saturation uptake at 30 kPa. The CO_2 desorption isotherm does not trace the adsorption one, and a remarkable hysteresis is revealed. This novel sorption isotherm is a typical sign for a non-porous to porous structural transformation, which occurs at a certain gate-opening pressure.

The adsorptive separation of C_2H_2 and CO_2 has attracted great interest. The reported C_2H_2/CO_2 uptake ratios are usually larger than unity since C_2H_2 has a larger quadrupole moment (i.e., larger interaction energy with the host).[35,48−52] However, **1′** cannot adsorb C_2H_2 at 195 K, giving a remarkably reverse C_2H_2/CO_2 selectivity or C_2H_2/CO_2 uptake ratios significantly smaller than unity. Comparing the molecular sizes and kinetic diameters of the gas molecules indicate that the sorption behaviors of **1′** cannot be simply attributed to the size effect, since H_2 is absolutely smaller than CO_2, and C_2H_2 is similar to CO_2. Alternatively, the difference in host−guest affinity should be more important. Obviously, compared to N_2, H_2, and C_2H_2, only CO_2 molecules can utilize their electronegative oxygen atoms to interact with the coordinatively unsaturated, oxophilic Na(I) ions, and consequently open the gates and diffuse into the channels.[53−55]

Conclusions

Combining alkali metal ions, Co(II), and isophthalate, five new heterometallic carboxylate frameworks have been synthesized by solvothermal reactions in H_2O/alchohol mixed solvents. The anionic, square-grid $[Co(ipa)_2]_n$ network behaves as a robust building unit, which can be connected by alkali metal ions in various fashions to build neutral heterometallic carboxylate frameworks with different compositions and structures. Remarkable framework flexibility has been observed for the prototypical framework $[Na_2Co(ipa)_2]_n$, which is attributed to coordination flexibilities of the Co(II) and Na(I) ions, as well as the carboxylate groups. The representative compound of this framework, $[Na_2Co(ipa)_2(MeOH)_2]_n$, demonstrates multiple, solid-state structural transformations triggered by substitution and/or removal of the coordinated MeOH molecules. Although $[Na_2Co(ipa)_2(MeOH)_2]_n$ is non-porous in the as-synthesized state and after complete removal of all MeOH molecules, the resulting $[Na_2Co(ipa)_2]_n$ framework shows interesting sorption behaviors toward a variety of solvent vapors and gases. It is shown that the Na(I) ions is not only useful for binding oxygen containing solvent molecules but also for weaker ligands such as acetonitrile. While the different sorption properties for solvent vapors can be readily explained by the sizes of guest molecules, the selective gas sorption behaviors should be attributed to the difference between host−guest binding abilities.

Acknowledgment. This work was supported by the Chinese Ministry of Education (Grant 109125) and Kitagawa Integrated Pore Project, Exploratory Research for Advanced Technology (ERATO), Japan Science and Technology Agency (JST).

Supporting Information Available: Additional plots, TGA, and XRPD patterns (PDF), and X-ray data files (CIF). This material is available free of charge via the Internet at http://pubs.acs.org.

(48) Matsuda, R.; Kitaura, R.; Kitagawa, S.; Kubota, Y.; Belosludov, R. V.; Kobayashi, T. C.; Sakamoto, H.; Chiba, T.; Takata, M.; Kawazoe, Y.; Mita, Y. *Nature* **2005**, *436*, 238–241.
(49) Thallapally, P. K.; Dobrzańska, L.; Gingrich, T. R.; Wirsig, T. B.; Barbour, L. J.; Atwood, J. L. *Angew. Chem., Int. Ed.* **2006**, *45*, 6506–6509.
(50) Samsonenko, D. G.; Kim, H.; Sun, Y.; Kim, G.-H.; Lee, H.-S.; Kim, K. *Chem. Asian J.* **2007**, *2*, 484–488.
(51) Tanaka, D.; Higuchi, M.; Horike, S.; Matsuda, R.; Kinoshita, Y.; Yanai, N.; Kitagawa, S. *Chem. Asian J.* **2008**, *3*, 1343–1349.
(52) Zhang, J.-P.; Chen, X.-M. *J. Am. Chem. Soc.* **2009**, *131*, 5516.
(53) Chen, B.-L.; Ma, S.-Q.; Zapata, F.; Fronczek, F. R.; Lobkovsky, E. B.; Zhou, H.-C. *Inorg. Chem.* **2007**, *46*, 1233.
(54) Chen, B.-L.; Ma, S.-Q.; Hurtado, E. J.; Lobkovsky, E. B.; Zhou, H.-C. *Inorg. Chem.* **2007**, *46*, 8490.
(55) Li, J.-R.; Kuppler, R. J.; Zhou, H.-C. *Chem. Soc. Rev.* **2009**, *38*, 1477.